Korean J. Chem. Eng., 36(5), 660-668 (2019)
DOI: 10.1007/s11814-019-0253-7

pISSN: 0256-1115
eISSN: 1975-7220

Decomposition of ammonium dinitramide-based liquid propellant over Cu/hexaaluminate pellet catalysts

Sujeong Heo*, Munjeong Kim*, Jeongsub Lee, Young Chul Park**, and Jong-Ki Jeon*,†**

*Department of Chemical Engineering, Kongju National University, Cheonan 31080, Korea
**Agency for Defense Development, Daejeon 34186, Korea
(*Received 19 December 2018 • accepted 5 March 2019*)

Abstract−We investigated the influence of a copper loading strategy over hexaaluminate on catalytic performance during the decomposition of an ammonium dinitramide (ADN)-based liquid propellant. Powder-type and pellet-type Cu/hexaaluminate catalysts were prepared and their chemico-physical properties were characterized by N2 adsorption, XRD, and XRF. A Cu-hexa-pellet-A catalyst in which copper atoms are positioned inside the hexaaluminate matrix showed the lowest decomposition onset temperature in decomposition of an ADN-based propellant. The excellent activity of the Cu-hexa-pellet-A catalyst is ascribed to copper being well incorporated in the hexaaluminate matrix, and the dispersion of the copper is higher than that in two other catalysts. When a thermal shock was applied at a high temperature of 1,200 °C prior to catalyst reuse, physical properties such as surface area, average pore diameter, and the compressive strength of the fresh catalyst did not deteriorate remarkably after five times repetitive reuse and heat treatment. Consequently, the Cu-hexa-pellet-A catalyst was confirmed to be a catalyst that has excellent activity and heat resistance simultaneously in decomposition of an ADN-based propellant.

Keywords: Cu/Hexaaluminate, Pellet-type Catalyst, Ammonium Dinitramide, Propellant, Decomposition

INTRODUCTION

Liquid propellants are generally used in thrusters for attitude control in spacecraft, such as space launch vehicles and satellites, because liquid propellants can generate propulsion force for the rocket. Over the recent decades, hydrazine has been widely used as a liquid propellant in the aerospace industry; however, human health and handling hazards have become serious issues because hydrazine is very toxic and shows corrosive properties to human tissues. As a result, studies for developing eco-friendly liquid propellants with low toxicity have attracted much attention recently [1-4]. Ammonium dinitramide (ADN, $NH_4N(NO_2)_2$) is being studied as a major component of eco-friendly liquid propellants that can replace hydrazine [5,6]. ADN, composed of an ammonium ion (NH_4^+) and dinitramide ion ($N(NO_2)^{2-}$), has high nitrogen and oxygen content, making it suitable for new explosives, detonators, and rocket propellants [7-10]. Moreover, it does not generate halogen acid as a decomposition product, and has low flammability, high thrust, and good storage stability.

The ADN-based liquid propellant consists of ADN, water, methanol, and ammonia, which is known as 'LMP 103S' [11]. Previously, it was reported that there are seven decomposition pathways, Eqs. (1)-(7) for ADN-based liquid propellant as follows [11]:

$$NH_4N(NO_2)_2 \rightarrow NH_4NO_3+N_2O \quad (1)$$

$$NH_4NO_3 \rightarrow N_2O+2H_2O \quad (2)$$

$$NH_4NO_3 \rightarrow 3/4N_2+1/2NO_2+2H_2O \quad (3)$$

$$CH_3OH+NO_2 \rightarrow HCOOH+1/2N_2+H_2O \quad (4)$$

$$N_2O \rightarrow N_2+1/2O_2 \quad (5)$$

$$CH_3OH+O_2 \rightarrow HCOOH+H_2O \quad (6)$$

$$HCOOH+1/2O_2 \rightarrow CO_2+H_2O \quad (7)$$

The ADN-based liquid propellant has a disadvantage that ignition becomes difficult because of the high water content in the liquid propellant [9]. Once an ADN-based liquid propellant is sufficiently heated to above the specified temperature, known as the "decomposition onset temperature," in the thruster, explosive decomposition occurs. However, because the storage space of the energy source is limited within the satellite, energy consumption should be minimized. To meet these constraints, the decomposition onset temperature should be reduced as much as possible by catalytic decomposition; therefore, it is essential to develop effective catalysts capable of promoting the decomposition of an ADN-based liquid propellant at low temperatures. On the other hand, when the liquid propellant begins to decompose in satellite thrusters, the temperature of the catalyst bed rises to more than 1,200 °C [11,12]. Because the decomposition of the propellant occurs intermittently and repeatedly in satellite thrusters, a catalyst having high heat resistance is essential. That is, the catalyst used for decomposing the liquid propellant in the satellite thruster must have both high activity at low temperature and high heat resistance.

Platinum, iridium, rhodium, and copper have been studied as active metals for the decomposition of ADN-based liquid propellants [12-14]. Recently, hexaaluminate has been adapted as a cata-

†To whom correspondence should be addressed.
E-mail: jkjeon@kongju.ac.kr

lyst for high-temperature reactions such as catalytic combustion, partial oxidation, reforming, and N_2O decomposition reactions [15-17]. Hexaaluminate reportedly has high heat resistance even at 1,200 °C or higher [18,19]. It consists of a hexagonal aluminate compound with a unique layer structure of a dense oxide layer and a spinel block with a layered mirror surface. It has the general formula of $AB_xAl_{12-x}O_{19}$, in which A is a large cation such as Na, Sr, La, or Ba and B is a transition metal such as Mn, Fe, Co, Cu, or Ni [20,21].

When a catalyst is applied for decomposing a liquid propellant in a thruster, a catalyst body is necessarily required to minimize the pressure drop, and a powder type catalyst is not appropriate. Although catalysis in decomposition of liquid propellants is now an intensively studied discipline, there is scant knowledge about catalyst foaming, the success of which ultimately decides the overall feasibility of a decomposition process. Despite the importance of catalyst preparation procedures in the field of industrial catalysts for the decomposition of propellants, the influence of catalyst manufacturing strategy on catalytic performance has been underestimated. To the best of our knowledge, this study is the first to elucidate the foaming procedure for a pellet-type catalyst in the decomposition process of a liquid propellant.

The aim of this study was to determine the influence of a copper incorporation strategy over Sr-hexaaluminate on the catalytic performance during the decomposition of an ADN-based liquid propellant. After synthesis of a powder-type catalyst, a binder was added and the catalyst extruded into pellet form. Pellet type catalysts were calcined at 1,200 °C, and their physical and chemical properties were analyzed. In particular, this study focused on heat resistance of the pellet-type catalysts, and decomposition of the ADN-based liquid propellant was carried out to investigate the heat resistance and decomposition activity.

EXPERIMENTAL DETAILS

1. Synthesis of Hexaaluminate Powder

Sr-hexaaluminate composed of $Sr_{0.8}La_{0.2}MnAl_{11}O_{19}$ was prepared by a coprecipitation method [22,23]. A precursor solution was prepared by adding nitrates of strontium, lanthanum, manganese, and aluminum to deionized water. The precursor solution and ammonium hydroxide were added dropwise to an ammonium carbonate solution to precipitate the solution while maintaining the temperature at 60 °C and the pH at 7-8. After completing the precipitation step, aging, filtering, and drying were conducted and the precipitates was then calcined at 1,200 °C for four hours to prepare the hexaaluminate powder.

2. Preparation of Copper-incorporated Pellet-type Catalysts

The copper-incorporated catalysts were prepared using four methods. With the first method, $Cu(NO_3)_2$ was used during the synthesis of Sr-hexaaluminate powder through a coprecipitation method so that copper atoms could be positioned inside the hexaaluminate matrix. The powder was dried in an oven at 110 °C for 24 hours, and subsequently calcined at 1,200 °C for four hours. The as-prepared powder is referred to here as "Cu-hexa-powder".

As a second method, the Cu-hexa-powder was mixed with an organic binder (methyl cellulose, 5 wt%), an inorganic binder (montmorillonite, 50 wt%), and water. Subsequently, a pellet-type catalyst with a diameter of 2 mm and a length of 3 mm was prepared by extrusion of the mixture. The pelletized catalyst was calcined at 1,200 °C for 4 hours to complete the "Cu-hexa-pellet-A" catalyst (Fig. 1).

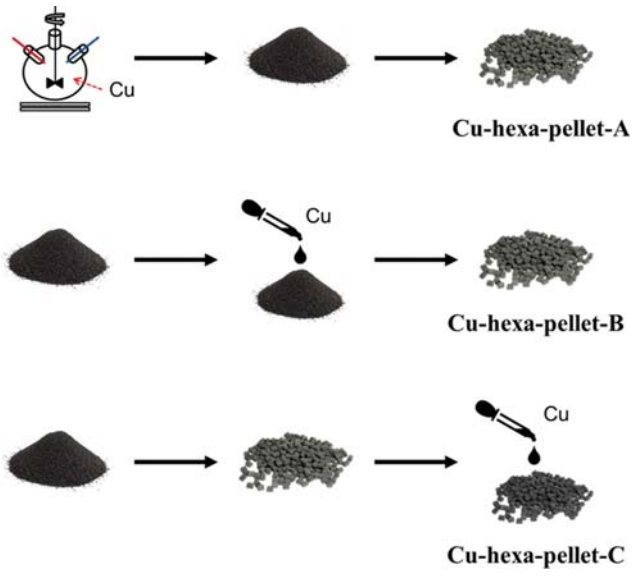

Fig. 1. Strategy of catalyst foaming.

In the third method, Cu (10 wt%) was impregnated on the Sr-hexaaluminate powder by incipient wetness method. Subsequently, extrusion was carried out after adding the organic and inorganic binders to prepare the pellet-type catalyst (2 mm in diameter and 3 mm in length). The prepared pellet-type catalyst was calcined at 1,200 °C for four hours to complete the catalysis of the Cu/Sr-hexaaluminate pellet; this was termed "Cu-hexa-pellet-B" (Fig. 1).

In the fourth method, a mixture of Sr-hexaaluminate powder and the organic and inorganic binders was initially formed into a pellet (2 mm in diameter and 3 mm in length) through extrusion. Then, Cu (10 wt%) was impregnated into the pellet using the incipient wetness method. The prepared pellet-type catalyst was calcined at 1,200 °C for four hours, and it was termed "Cu-hexa-pellet-C" (Fig. 1).

3. Characterization of the Catalysts

An N_2 adsorption-desorption analysis was carried out at the liquid nitrogen temperature using a BELSORP II device from BEL Japan, Inc. The specific surface area of the catalyst was calculated using the Brunauer-Emmett-Teller (BET) method, and the total pore volume was checked by calculating the amount of condensed nitrogen at P/P_0=0.99 using the Barrett-Joyner-Halenda (BJH) method. For X-ray diffraction (XRD) analysis, a Rigaku MiniFlex600 device (600 W, 40 kV, 15 mA), which uses Ca Kα radiation as an X-ray source, was used. The compositions of the prepared catalyst were analyzed in accordance with the X-ray fluorescence with a Primus model from Rigaku. The scanning electron microscope - energy dispersive X-ray spectroscopy (SEM-EDS) was utilized to study the surface morphology of the catalysts using the MIRA LMH model from Tescan. The compressive strength of the catalyst pellet was measured using a DS2-200N model of IMADA. The com-

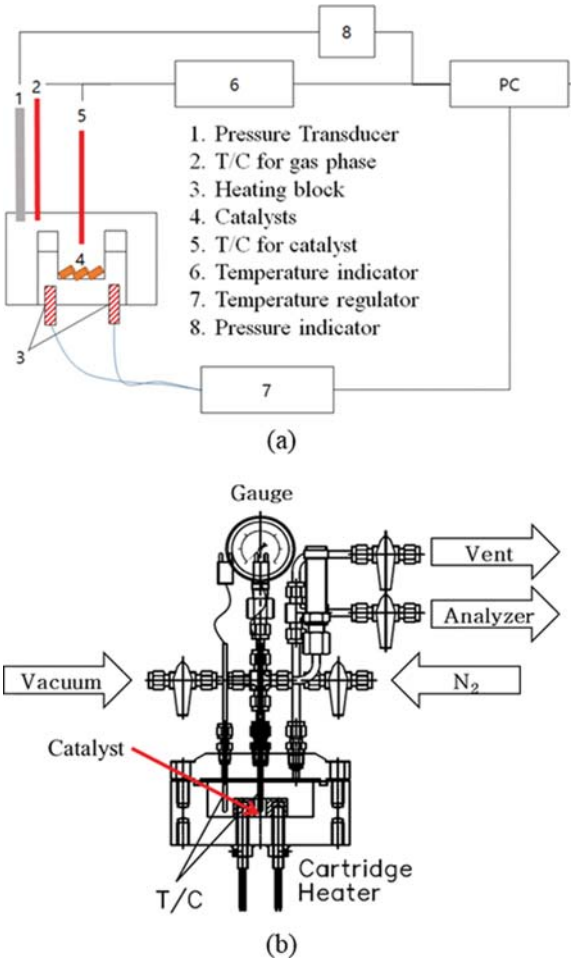

Fig. 2. Schematic diagram of apparatus for decomposition of propellant.

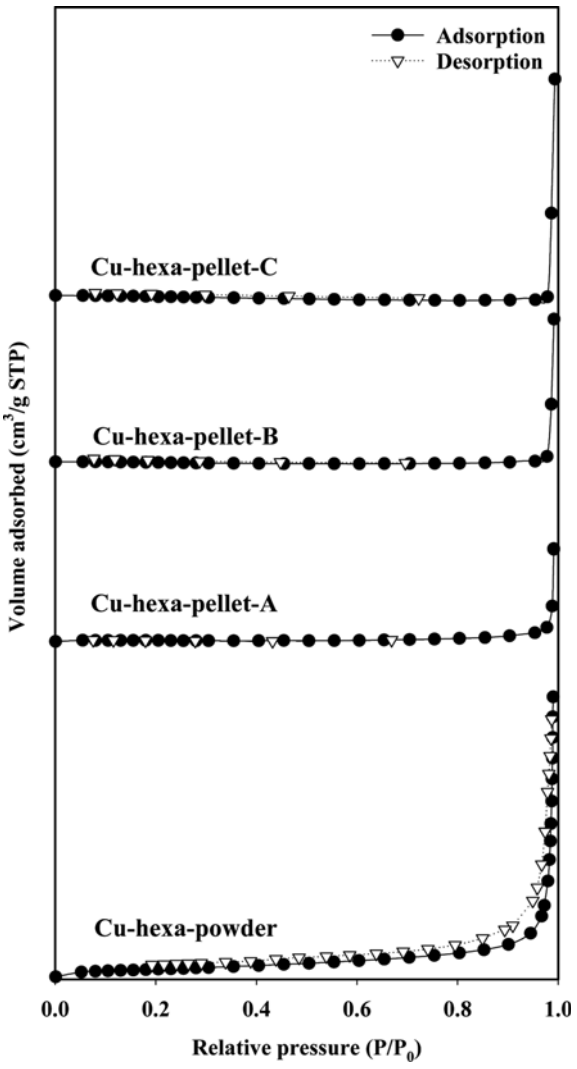

Fig. 3. N_2 adsorption isotherm of various catalysts.

pressive strength was determined by dividing the compressive load when the catalyst pellet was broken by the cross-sectional area of the catalyst pellet.

4. Catalytic Decomposition of the Liquid Propellant

The ADN-based liquid propellant used in this study was composed of 65 wt% of ADN, 10 wt% of methanol, 10 wt% of water, and 5 wt% of ammonia. The decomposition reaction of the ADN-based liquid propellant was carried out inside a semi-batch reactor fabricated in-house. After inputting 80 mg of the catalyst and 50 μL of ADN-based liquid propellant into the reactor, the temperature and pressure inside the reactor were measured ten times per second while increasing the temperature at a rate of 10 °C/min. The temperature at which the temperature and pressure abruptly increased because the decomposition of the ADN-based liquid propellant was set as the decomposition onset temperature. The product stream was collected using Tedlar bag and analyzed using an infrared spectrometer (Nicolet iS50 FT-IR).

RESULTS AND DISCUSSION

1. Characteristics of the Catalysts

The N_2 adsorption isotherms of the three types of pellet catalysts (Fig. 3) show that they correspond to Type III in the IUPAC classification, meaning that the adsorbed molecules are clustered around the most favorable sites on the surface of a nonporous or macroporous solid and the micropores are mostly undeveloped [24]. The BET surface areas of the Cu-hexa-powder, Cu-hexa-pellet-A, Cu-hexa-pellet-B, and Cu-hexa-pellet-C catalysts were measured to be 4.0, 0.3, 0.6, and 1.1 m^2/g, respectively (Table 1), which indicates that the surface area is drastically reduced through the foaming procedure in comparison with the powder-type catalyst. This is attributed to the pelletized catalysts containing inorganic binders and being calcined at a high temperature of 1,200 °C. The order of the surface area and pore volume is Cu-hexa-pellet-C>Cu-

Table 1. BET surface area and total pore volume of various catalysts

Catalyst	S_{BET} (m^2/g)	V_p (cm^3/g)
Cu-hexa-powder	4.0	0.030
Cu-hexa-pellet-A	0.3	0.010
Cu-hexa-pellet-B	0.6	0.015
Cu-hexa-pellet-C	1.1	0.023

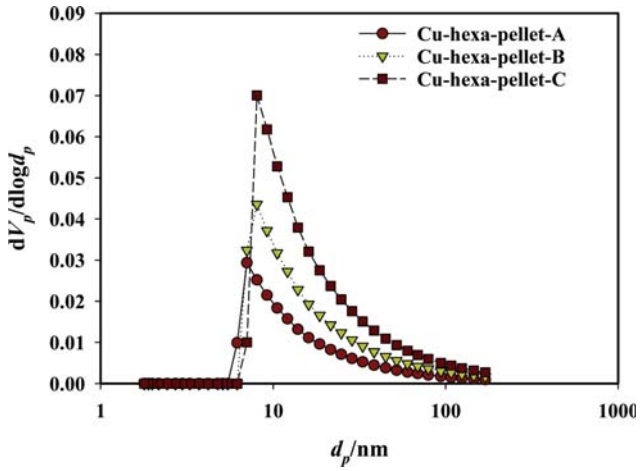

Fig. 4. Pore size distribution of various catalysts.

hexa-pellet-B>Cu-hexa-pellet-A, and the surface area and pore size of Cu-hexa-pellet-C are about four times those of Cu-hexa-pellet-A. It was also found that all three types of pellet catalysts developed mesopores in accordance with the pore size distribution measured using the BJH method (Fig. 4). The average pore size of the three types of pellet catalysts is about the same at about 10 nm.

The XRD patterns of the catalysts are shown in Fig. 5. The Cu-hexa-powder catalyst shows an XRD pattern very similar to that of hexaaluminate without copper, indicating that the Cu-hexa-powder catalyst prepared by the co-precipitation method including the Cu precursor retains the hexaaluminate structure well [19,25,26]. In the case of the Cu-hexa-pellet-A catalyst, the hexaaluminate structure can be confirmed because most characteristic peaks of the hexaaluminate structure are shown, although the XRD pattern is more complicated because of the characteristic peak of the inorganic binder (M). However, the XRD patterns of the Cu-hexa-pellet-B catalyst and the Cu-hexa-pellet-C catalyst were very different from the XRD pattern of the hexaaluminate and confirmed to be mostly because of the peaks of the copper oxide, α-alumina, and inorganic binder. That is, the Cu-hexa-pellet-B catalyst and the Cu-hexa-pellet-C catalyst are considered to correspond to the alumina structure rather than the hexaaluminate structure.

The composition of the catalysts was confirmed by XRF analysis (Table 2). For the Cu-hexa-pellet-A sample, Sr was more distributed than Cu, indicating that Cu was present inside the hexaaluminate matrix as opposed to being on the surface of the catalyst. The Cu-hexa-pellet-A sample contains a larger amount of alumina than the Cu-hexa-powder sample because the Cu-hexa-pellet-A contains a large amount of inorganic binders. However, in the Cu-hexa-pellet-B and Cu-hexa-pellet-C cases, there was much more copper present on the surface compared with the Cu-hexa-powder catalyst. Because Cu-hexa-pellet-B and Cu-hexa-pellet-C were prepared with hexaaluminate first for use as a support and then copper impregnated onto the support, a relatively large amount of copper was exposed on the surface of the pellet-type catalyst.

The presence of Cu on the surface of the catalysts was confirmed with SEM-EDS spectroscopy (Fig. 6). Copper particles (green color) on the Cu-hexa-pellet-A sample show better dispersion at smaller

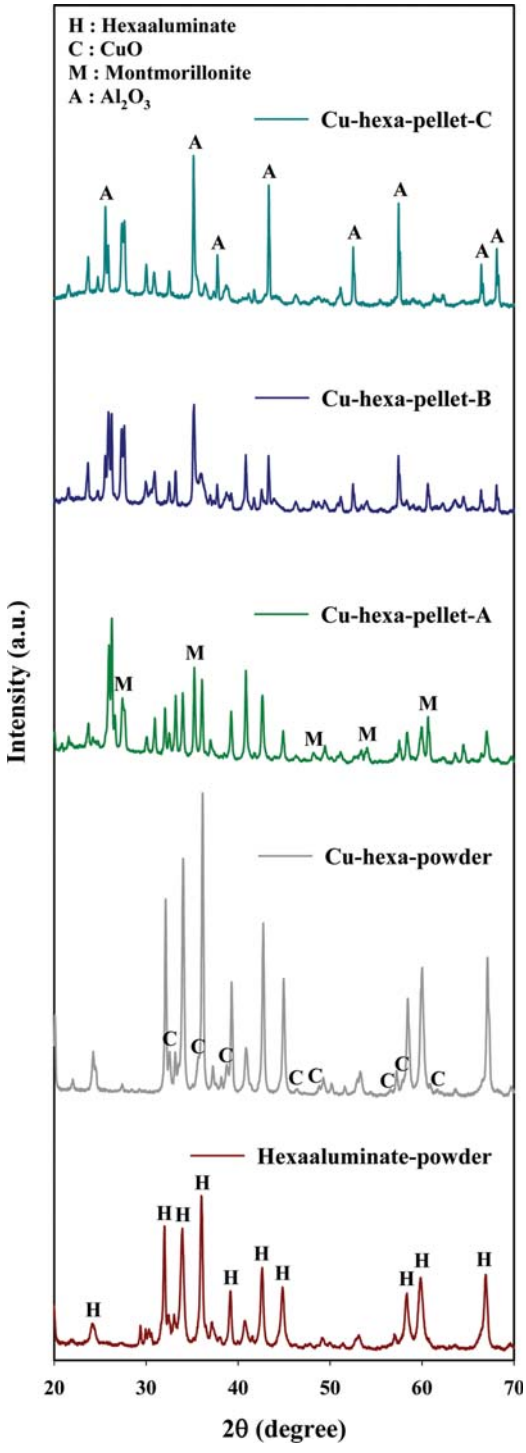

Fig. 5. XRD patterns of various catalysts.

Table 2. Composition of various catalysts determined by XRF

Catalyst	SrO (wt%)	La_2O_3 (wt%)	MnO (wt%)	Al_2O_3 (wt%)	CuO (wt%)
Cu-hexa-powder	45.6	11.5	6.7	17.4	18.8
Cu-hexa-pellet-A	29.2	7.2	5.1	47.9	10.6
Cu-hexa-pellet-B	24.6	5.0	8.6	36.7	25.1
Cu-hexa-pellet-C	19.5	4.1	6.6	30.3	39.5

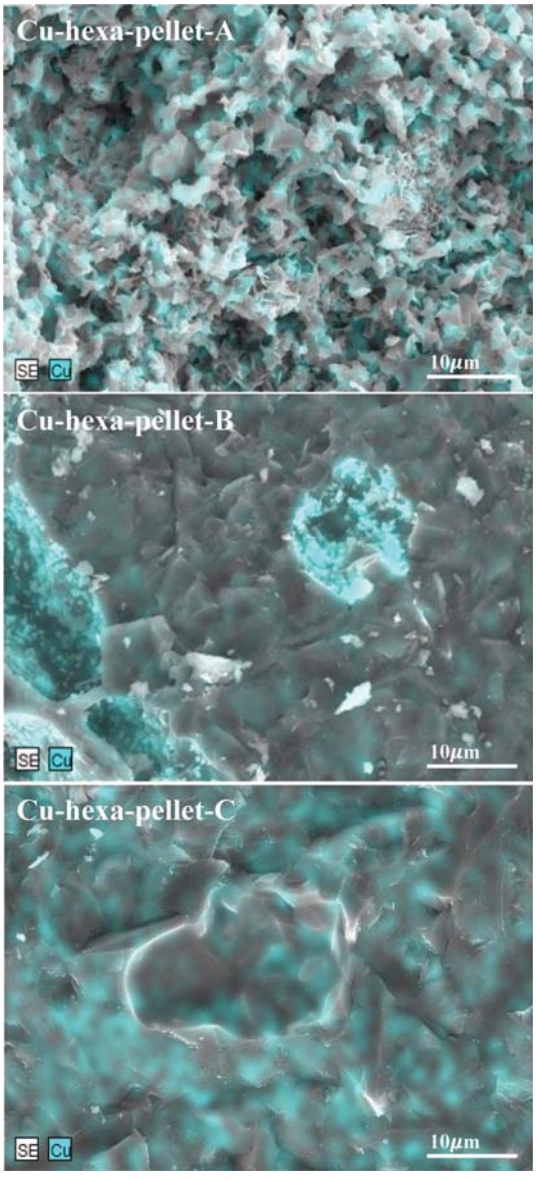

Fig. 6. SEM-EDS images of various catalysts.

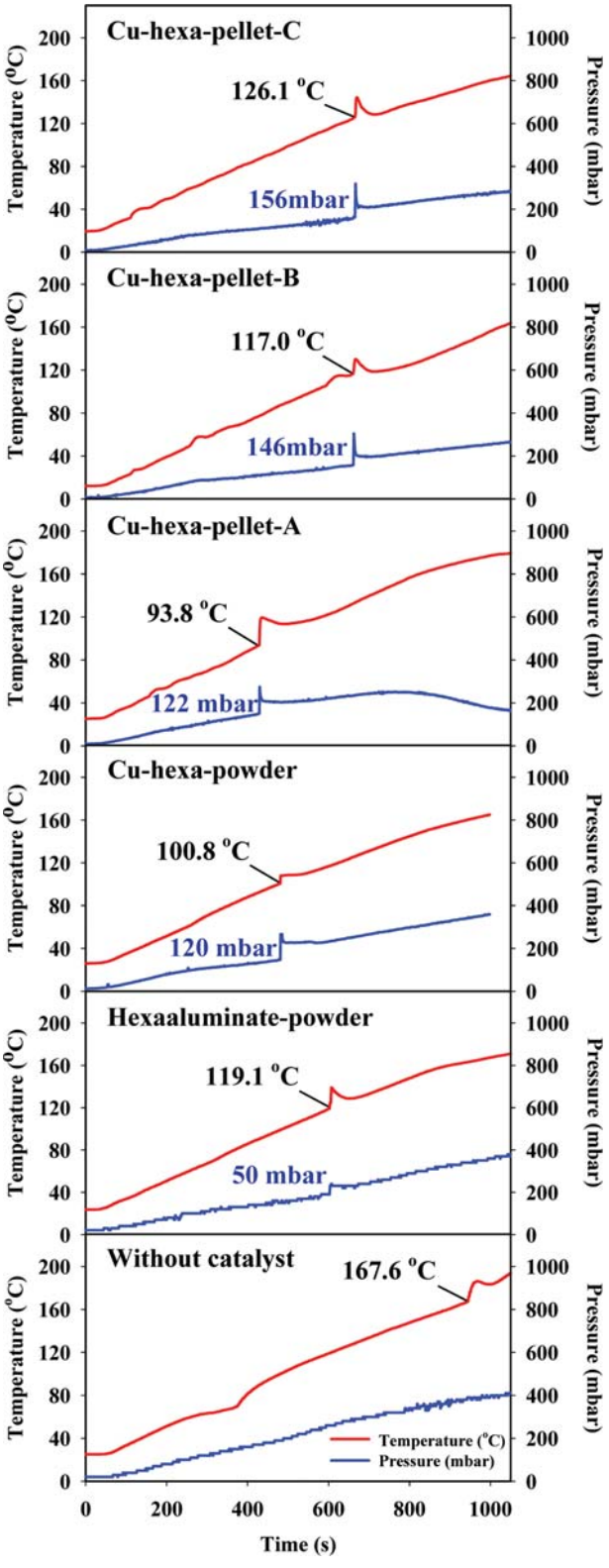

Fig. 7. Temperature and pressure record vs. time during decomposition of ADN-based monopropellant.

sizes than the other two catalysts. Copper dispersion of catalysts can also be compared with XRD analysis (Fig. 5). Scherrer's equation was used to calculate the mean crystallite size of copper oxide. The mean crystallite size of copper was found to be 32.0, 34.4 and 40.4 nm over the Cu-hexa-pellet-A, Cu-hexa-pellet-B, and Cu-hexa-pellet-C catalysts, respectively. From the results of XRD and SEM-EDS spectroscopy, it was found that copper was most well dispersed on the Cu-hexa-pellet-A catalyst among the three catalysts prepared in this study.

2. Catalytic Decomposition of the Liquid Propellant

The catalytic performance during the decomposition of the ADN-based liquid propellant is presented in Fig. 7. First, it was confirmed that the ADN-based liquid propellant was decomposed in one step by catalytic decomposition as well as by thermal decomposition. During the decomposition of the ADN-based liquid propellant, the temperature of the catalyst increased sharply because of a strong exothermic reaction. The point at which the temperature started to increase is referred to as the decomposition onset temperature [8,9]. In addition, the gas product formed abruptly during the de-

Table 3. BET surface area and total pore volume of the fresh and used catalysts

Catalyst	S_{BET} (m^2/g)	V_p (cm^3/g)
Cu-hexa-pellet-A-fresh	0.3	0.010
Cu-hexa-pellet-A (after 5 times decomposition reaction without thermal shock)	0.4	0.011
Cu-hexa-pellet-A (after 5 times decomposition reaction with thermal shock)	0.4	0.008

composition process, and this was accompanied by an abrupt pressure increase. The difference at this time between the pressure just before decomposition and the maximum pressure is expressed as ΔP. The lower the decomposition onset temperature, the better the catalytic activity in the decomposition of the ADN-based liquid propellant [4,8,9].

In the thermal decomposition without a catalyst in the decomposition reaction of the ADN-based liquid propellant, the decomposition onset temperature was 167.6 °C. During the decomposition using catalysts, the decomposition onset temperature was much lower. For decomposition using the Cu-hexa-pellet-A, Cu-hexa-pellet-B, and Cu-hexa-pellet-C, the decomposition onset temperatures were 93.8 °C, 117.0 °C, and 126.1 °C, respectively. For decomposition using the Cat-C-pellet catalyst, in which hexaaluminate was formed into a pellet and where copper was impregnated during the last stage, the decomposition onset temperature of 126.1 °C is similar to that of a $CuMnO_x$ catalyst [13]. The Cu-hexa-pellet-A showed the lowest decomposition onset temperature, with the decomposition onset temperature being lowered by 73.8 °C compared with that of thermal decomposition. This means that the Cu-hexa-pellet-A catalyst showed excellent decomposition activity and was the best among the catalysts tested here. Also, the Cu-hexa-pellet-A catalyst has the smallest specific surface area (Table 1). Furthermore, as confirmed from the XRF analysis results (Table 2), the number of copper atoms present on the surface of the Cu-hexa-pellet-A catalyst is much smaller than that of the Cu-hexa-pellet-B and Cu-hexa-pellet-C catalysts. Therefore, the pore structure and the copper content of the catalyst surface cannot account for the excellent activity of the Cu-hexa-pellet-A catalyst. XRF analysis shows that the Cu-hexa-pellet-A catalyst maintained the hexaaluminate structure, while the Cu-hexa-pellet-B and Cu-hexa-pellet-C catalysts did not retain the hexaaluminate structure (Fig. 5). Therefore, it is deduced that the excellent activity of the Cu-hexa-pellet-A catalyst is due to the hexaaluminate structure. In the case of the Cu-hexa-pellet-A catalyst, copper is well incorporated in the hexaaluminate matrix and the dispersion of the copper is higher than in the other two catalysts.

The product gases collected from the catalytic decomposition of the ADN-based liquid propellant over the the Cu-hexa-pellet-A catalyst was analyzed using infrared spectrometer as shown in Fig. 8. FT-IR absorbance bands due to NH_4NO_3, HCOOH, N_2O, and NO_2 were observed, which well corresponded to the previous report on the decomposition mechanism of LMP 103S [11].

To verify the reusability of the Cu-hexa-pellet-A catalyst, ADN-based propellant decomposition experiments were repeated five times (Fig. 9). During the five-times repetitive decomposition of the ADN-based propellant, the decomposition onset temperature and the ΔP were maintained at a constant level. The N_2 adsorption isotherm and pore size distribution of the spent catalysts after five repetitive decomposition experiments did not show any considerable differences from those of the fresh catalysts (Fig. 10 and Fig. 11, respectively). Accordingly, the surface area and pore volume of the Cu-hexa-pellet-A catalyst did not decrease after repeated decomposition reactions. Moreover, the compressive strength of the used pellet catalyst was similar to that of a fresh pellet catalyst (Fig. 12). As a result, it was confirmed that the Cu-hexa-pellet-A catalyst could be recovered and reused as a catalyst for decomposition of an ADN-based propellant.

When an ADN-based propellant is used as fuel in a satellite thruster, the temperature of the catalyst bed is known to rise intermittently and repeatedly up to 1,200 °C. To measure the heat resis-

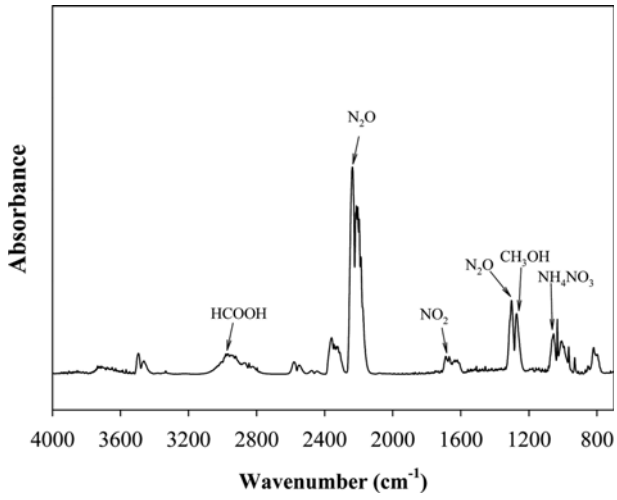

Fig. 8. FT-IR spectra for the decomposition product gases from ADN-based monopropellant in the presence of Cu-hexa-pellet-A catalyst.

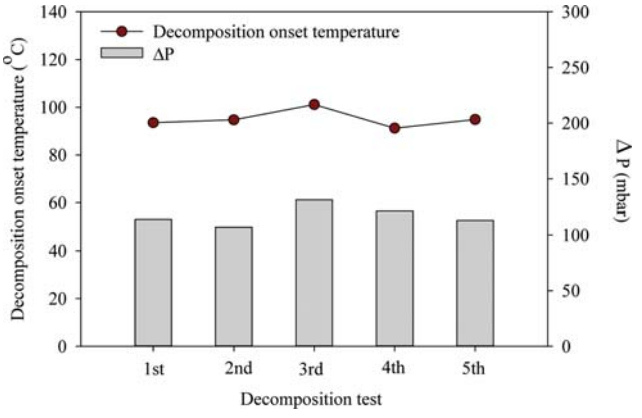

Fig. 9. Decomposition onset temperature and pressure drop during decomposition of ADN-based monopropellant over Cu-hexa-pellet-A catalyst for five repetitive tests.

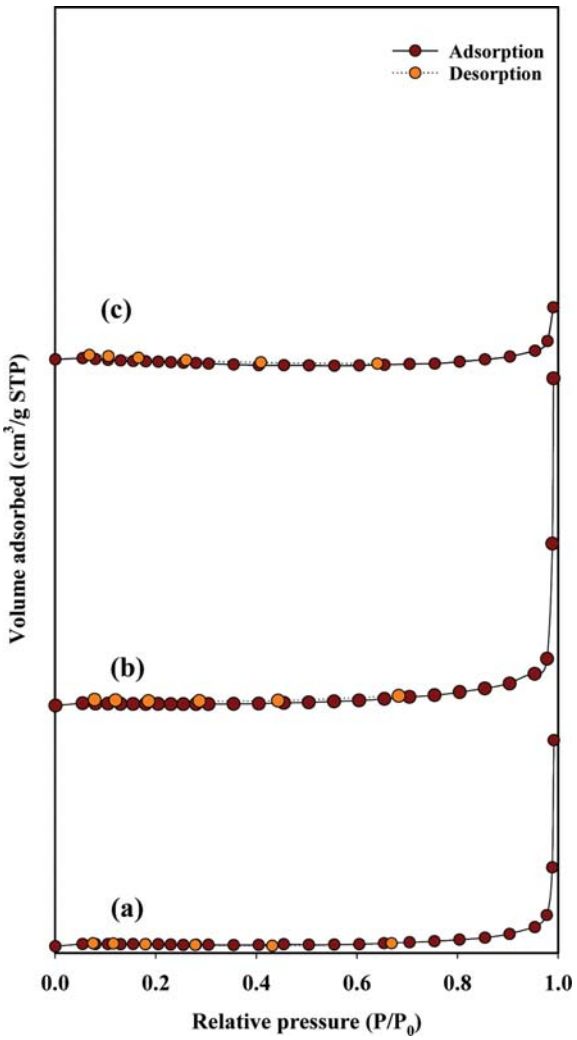

Fig. 10. N_2 adsorption isotherms of Cu-hexa-pellet-A catalysts: (a) Fresh catalyst, (b) used catalyst after five repetitive tests without thermal shock, (c) used catalyst after five repetitive tests with thermal shock.

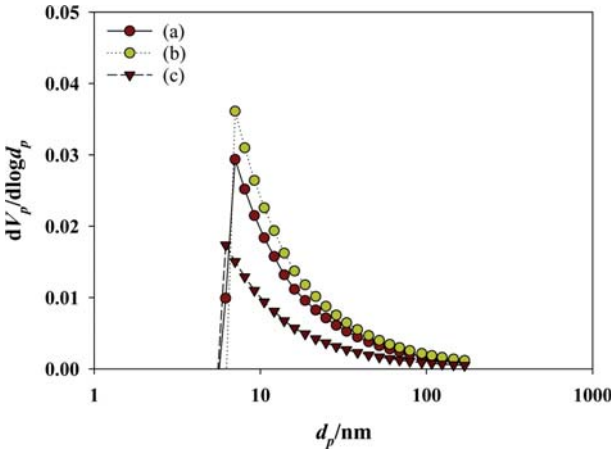

Fig. 11. Pore size distributions of Cu-hexa-pellet-A catalysts: (a) Fresh catalyst, (b) used catalyst after five repetitive tests without thermal shock, (c) used catalyst after five repetitive tests with thermal shock.

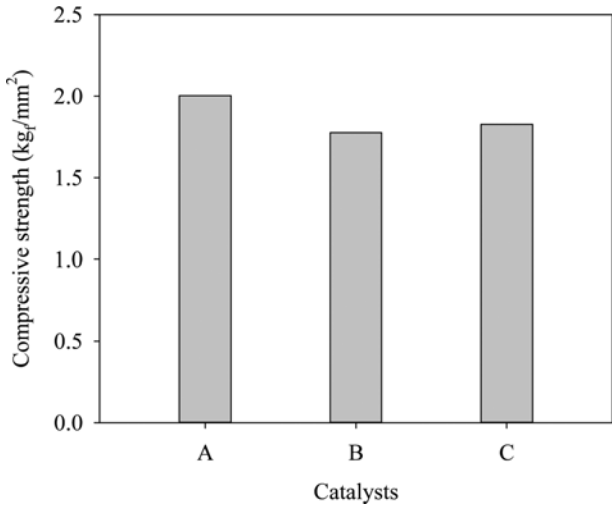

Fig. 12. Compressive strength of Cu-hexa-pellet-A catalysts: (a) Fresh catalyst, (b) used catalyst after five repetitive tests without thermal shock, (c) used catalyst after five repetitive tests with thermal shock.

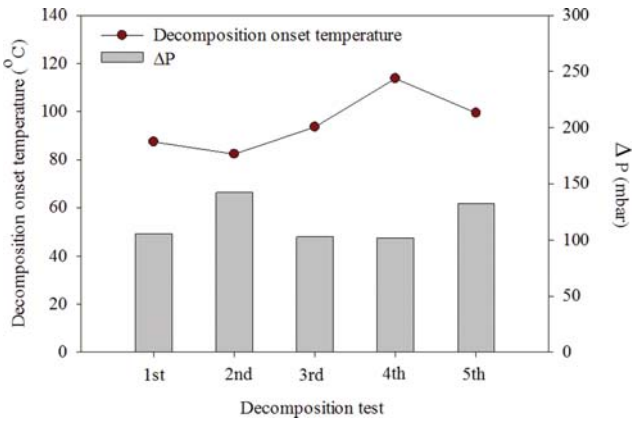

Fig. 13. Decomposition onset temperature and pressure drop during decomposition of ADN-based monopropellant over Cu-hexa-pellet-A catalyst for five repetitive tests with thermal shock.

tance of the Cu-hexa-pellet-A catalyst under more severe conditions, the catalyst was recovered and heat treated at 1,200 °C for 10 minutes prior to reuse. The catalytic activity did not decrease remarkably after five repeated experiments, even when a thermal shock was applied at a high temperature of 1,200 °C prior to catalyst reuse (Fig. 13). It was confirmed that physical properties such as surface area, average pore diameter, and the compressive strength of the fresh catalyst did not deteriorate remarkably after five-times repetitive reuse and heat treatment. SEM images before and after decomposition experiments are shown in Fig. 14. It was difficult to find the change of particle texture between the fresh and spent catalysts. Even after a thermal shock at 1,200 °C, there was no significant change in the structure of the catalyst. Consequently, the Cu-hexa-pellet-A catalyst was confirmed to be a catalyst that has excellent activity and heat resistance simultaneously in the decomposition of an ADN-based propellant.

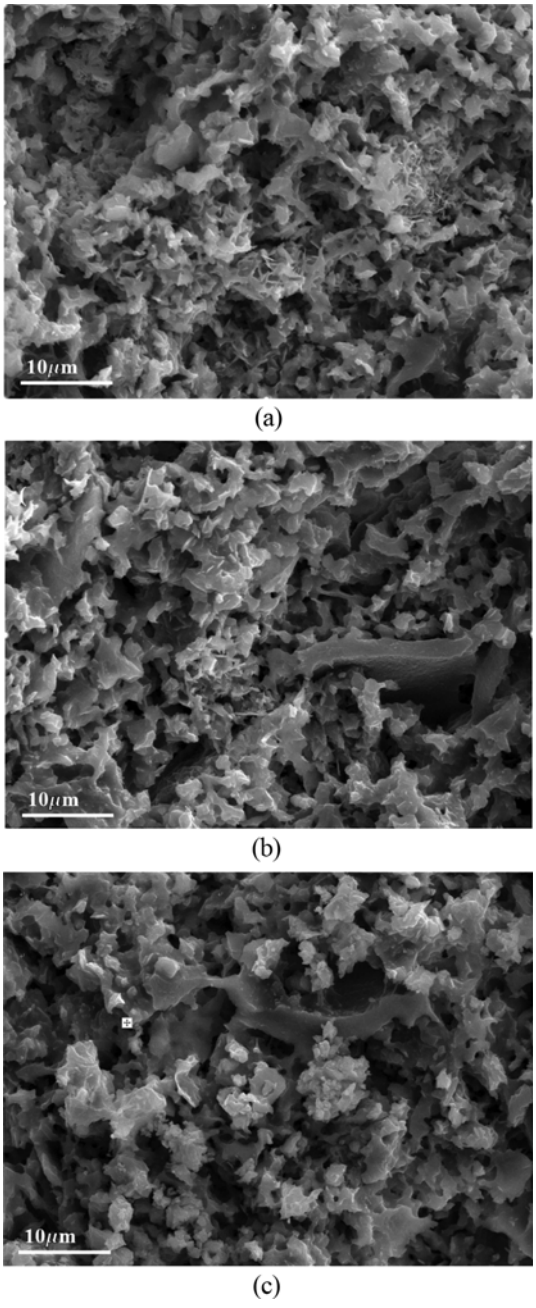

Fig. 14. SEM images of Cu-hexa-pellet-A catalysts: (a) Fresh catalyst, (b) used catalyst after five repetitive tests without thermal shock, (c) used catalyst after five repetitive tests with thermal shock.

CONCLUSION

The Cu-hexa-pellet-A catalyst in which copper atoms are positioned inside the hexaaluminate matrix showed the lowest decomposition onset temperature in decomposition of an ADN-based propellant. The excellent activity of the Cu-hexa-pellet-A catalyst is ascribed to the copper being well incorporated in the hexaaluminate matrix, and the dispersion of the copper is higher than that in the other two catalysts. When a thermal shock was applied at a high temperature of 1,200 °C prior to catalyst reuse, physical properties such as surface area, average pore diameter, and the compressive strength of the fresh catalyst did not deteriorate remarkably after five times repetitive reuse and heat treatment. Consequently, the Cu-hexa-pellet-A catalyst was confirmed to be a catalyst that has excellent activity and heat resistance simultaneously in decomposition of an ADN-based propellant.

ACKNOWLEDGEMENTS

We acknowledge the financial support from the ADD fundamental project program.

REFERENCES

1. T. Nobuhiko, M. Tetsuya, F. Katsumi, N. Mitsuru, S. Shigenori and Y. Akinori, *Mitsubishi Heavy Ind. Tech. Rev.*, **48**, 44 (2011).
2. C. H. McLean, W. D. Deininger and J. Joniatis, 50th AIAA/ASME/SAE/ASEE Joint Propulsion Conference, AIAA 2014-3481, 1 (2014).
3. Y. Ide, T. Takahashi, K. Iwai, K. Nozoe, H. Habu and S. Tokudome, *Procedia Eng.*, **99**, 332 (2015).
4. R. Amrousse, T. Katsumi, N. Itouyama, N. Azuma, H. Kagawa, K. Hatai, H. Ikeda and K. Hori, *Combust. Flame*, **162**, 2686 (2015).
5. N. Wingborg, A. Larsson, M. Elfsberg and P. Appelgren, 41st AIAA/ASME/SAE/ASEE Joint Propulsion Conference & Exhibit, AIAA 2005-4468, 1 (2005).
6. H. G. Jang, M. J. Sul, J. S. Shim, Y. C. Park and S. J. Cho, *J. Ind. Eng. Chem.*, **63**, 237 (2018).
7. R. Yang, P. thakre and V. Yang, *Combust. Explo. Shock Waves*, **41**, 657 (2005).
8. J. Kleimark, R. Delanoë, A. Demairé and T. Brinck, *Theor. Chem. Acc.*, **132**, 1 (2013).
9. L. Courthéoux, D. Amariei, S. Rossignol and C. Kappenstein, *Appl. Catal. B: Environ.*, **62**, 217 (2006).
10. S. Vyazovkin and C. A. Wight, *J. Phys. Chem. A*, **101**, 5653 (1997).
11. T.-A. Gronland, B. Westerberg, G. Bergman, K. Anflo, J. Brandt, O. Lyckfeldt, J. Agrell, A. Ersson, S. Jaras, M. Boutonnet and N. Wingborg, US Patent, 7,137,244 B2 (2006).
12. R. Amrousse, K. Hori, W. Fetimii and K. Farhat, *Appl. Catal. B: Environ.*, **127**, 121 (2012).
13. S. Heo, S. Hong, B. K. Jeon, C. Li, J. M. Kim, Y. M. Jo, W. Kim and J.-K. Jeon, *J. Nanosci. Nanotechnol.*, **18**, 353 (2018).
14. S. Hong, S. Heo, C. Li, B. K. Jeon, J. M. Kim, Y. M. Jo, W. Kim and J.-K. Jeon, *J. Nanosci. Nanotechnol.*, **18**, 1427 (2018).
15. M. Machida, K. Eguchi and H. Arai, *J. Catal.*, **120**, 377 (1989).
16. R. W. Sidwell, H. Zhu, R. J. Kee and D. T. wickham, *Combust. Flame*, **134**, 55 (2003).
17. S. Hong, S. Heo, W. Kim, Y. M. Jo, Y. K. Park and J. K. Jeon, *Catalysts*, **9**, 80 (2019).
18. T. H. Gardner, D. Shekhawat, D. A. Berry, M. W. Smith, M. Salazar and E. L. Kugler, *Appl. Catal. A: Gen.*, **323**, 1 (2007).
19. M. Machida, K. Eguchi and H. Arai, *J. Catal.*, **123**, 477 (1990).
20. M. Tian, X. D. Wang and T. Zhang, *Catal. Sci. Technol.*, **6**, 1984 (2016).
21. L. Lietti, C. Cristiani, G. Groppi and P. forzatti, *Catal. Today*, **59**, 191 (2000).
22. B. W.-L. Jang, R. M. Nelson, J. J. Spivey, M. Ocal, R. Oukaci and G.

Mareclin, *Catal. Today*, **47**, 103 (1999).
23. T.-F. Yeh, H.-G. Lee, K.-S. Chu and C.-B. Wang, *Mater. Sci. Eng. A*, **384**, 324 (2004).
24. M. Thommes, K. Kaneko, A. V. Neimark, J. P. Olivier, F. Rodriguez-Reinoso, J. Rouquerol and K. S. W. Sing, *Pure Appl. Chem.*, **87**, 1051 (2015).
25. S. Kim, D.-W. Lee, J. Y. Lee, H.-J. Eom, H. J. Lee, I.-H. Cho and K.-Y. Lee, *J. Mol. Catal. A: Chem.*, **335**, 60 (2011).
26. J.-M. Son and S.-I. Woo, *Korean Chem. Eng. Res.*, **45**, 209 (2007).